Scientific Research Publishing

Open Journal of Geology, 2018, 8, 1146-1165
http://www.scirp.org/journal/ojg
ISSN Online: 2161-7589
ISSN Print: 2161-7570

Petrophysical Analysis and Flow Units Characterization for Abu Madi Pay Zones in the Nile Delta Reservoirs

Abdulaziz M. Abdulaziz*, Mohamed Metwally, A. S. Dahab

Faculty of Engineering, Cairo University, Giza, Egypt
Email: *amabdul@miners.utep.edu

How to cite this paper: Abdulaziz, A.M., Metwally, M. and Dahab, A.S. (2018) Petrophysical Analysis and Flow Units Characterization for Abu Madi Pay Zones in the Nile Delta Reservoirs. *Open Journal of Geology*, **8**, 1146-1165.
https://doi.org/10.4236/ojg.2018.812070

Received: December 12, 2017
Accepted: November 26, 2018
Published: November 29, 2018

Abstract

Field development typically requires detailed petrophysical analysis and well defined hydraulic flow units for comprehensive formation evaluation and reservoir characterization. In the present study, pay zones petrophysics are studied using an assembly of well log data from 8 wells together with core plugs measurements. Petrophysical analysis showed a good reservoir quality with average water saturation increasing toward the East and Southeast of the study area. Using a multi-linear regression technique on well logs and core data, permeability is estimated at well locations for flow unit characterization and flow capacity calculation. Results showed that five hydraulic flow units are identified through the studied wells, with relatively good correlation. Such correlation indicated a good continuity in the net pay zone of Abu Madi Formation in the Nile Delta reservoirs. The developed hydraulic flow units (HFUs) are classified according to its hydraulic conductivity into two main categories: the first category comprises the units with low permeability (K < 220 mD), and the second category involves the units with high permeability (K > 1270 mD). The reservoir flow capacity (RFC) of these units indicated the development of 4 distinct classes (~11, ~30, ~80, and greater than 130 D.ft). The wells within the Northwestern part of the study area showed three HFUs that relatively vary from those located at the Southeast where two HFUs are only developed. In addition, the Southeastern part of the reservoir is characterized by good RFC as indicated by the development of high order HFUs (3, 4, and 5) compared to the Northeastern part with predominated low order HFUs (1, 2, and 3). Such results are crucial for the efficient field development and profound reservoir management of oil and gas fields in the Nile Delta.

Keywords

Abu Madi, Formation Evaluation, Hydraulic Flow Units, Reservoir

Characterization, Flow Capacity

1. Introduction

Effective description for efficient reservoir characterization and the synergy of geological and engineering techniques are the key parameters for a comprehensive reservoir management [1]. Amaefule *et al.* [2], defined reservoir characterization as the combined efforts that discretize the reservoir geobody into subunits of suitable size such as layers and/or grid blocks with all physical properties assigned to each subunit. Typically, data from various sources including cores, logs, well test, and production data are utilized to describe the reservoir in terms of texture, fluid content, and hydraulic characteristics. Normally, the variation of measurement protocols greatly influences certain rock properties such as porosity, permeability, grain density, and capillary pressure that also vary with the change in geological factors such as the environment of deposition and diagenetic history [3]. Therefore, the efficient reserve calculations and improved reservoir productivity should not entirely use empirical correlations but rather adopt relationships based on core-derived parameters and well log measurements [2] [4]. In addition, the cut-offs play an important role in the realizations of the asset value, and consequently a properly conditioned set of petrophysical cut-offs for reservoir characterization. A better synergy between the static and dynamic reservoir models is an additional influential parameter to consider [5].

Permeability estimation is essential for reservoir modeling and development management due to its strong relation to the production rate [6]. In a general sense, permeability increases as porosity, grain size, and/or improved sorting increases [7] [8]. Geologists and reservoir engineers attempt to correlate the permeability via rock and fluid properties [9]. Thus, permeability prediction using rock properties should be developed for the zones that relatively share similar properties. Alternatively, Ebanks [10] introduced the term "flow unit" to subdivide the reservoir volume into a number of flow units based on geological and petrophysical properties that influence the fluids flow across the reservoir. This concept was later modified by Ebanks *et al.* [11] to involve a mappable portion of the total reservoir within which geological and petrophysical properties that affect fluids flow are consistent and predictably different from the properties of other reservoir rock volumes. In clastic rocks, these flow units are characterized hydraulically using flow zone indicator [2] as presented by References [12] and [13]. On contrast, in carbonates, rock fabrics are used as a characterization criterion that showed better correlation with pore structure and conductivity [6]. Due to the limited frequency and continuity of core data, permeability is usually estimated using well logs in mature fields.

Permeability prediction form static data can be grouped into two categories; pore (micro) scale as in core analysis and field (macro) scale as in well test. In

field scale category, various well log measurements are utilized rather than microscopic rock properties. Various forms of porosity-permeability correlation have been developed to provide a reasonable estimate to permeability from well logs [14] [15] [16] [17] and/or pore scale analysis [18] [19]. Permeability can be predicted using well log data and core permeability linear regression (single or multiple) analysis [20] [21], artificial neural-networks [22] [23], and decision tree [24]. Alternatively, in pore scale category, effective permeability can be approximated using specific calculated parameters such as porosity and irreducible water saturation as in Timur and Schlumberger models [25]. Recently, Mohammadmoradi and Kantzas [26] applied computational fluid dynamics and Direct Simulation Monte Carlo (DSMC) techniques to calculate pore-scale permeability. Generally, these models are dependent to the pore characteristics of the geobody including pore neck dimensions, pore size and the dominant petro-fabrics [6].

Of these numerous techniques, multilinear regression of log data seems simple and several studies indicated its potential application in permeability prediction for both clastic and carbonate reservoirs. Multiple Linear Regression (MLR) technique is applied to develop a correlation between permeability and independent parameters for a heterogeneous sandstone Formation [22] [27] [28] [29]. Saner *et al.* [30] applied a similar methodology for a carbonate reservoir, whereas Rios *et al.* [31] used principal component regressions of Nuclear Magnetic Resonance (NMR) and Mercury Injection Capillary Pressure (MICP) data to predict permeability of carbonate rocks. These successful applications proved that it is possible to apply the MLR for the development of permeability correlations to the Abu Madi Formation. Abu Madi Formation represents the main gas producing horizon in the Nile Delta and is made of a marine series of Lower Pliocene thick sand bodies that is in part pebbly or sporadically enclose thin shale interbeds. The shale content increases upward to change the facies into the overlying Kafr El Sheikh Formation showing a typical gradational contact [32]. Such variation in facies correlates with the change in the depositional environment from deltaic (Abu Madi) to shallow marine (Kafr El Sheikh). Detailed sequence stratigraphy framework of Abu Madi and Qawasim Formation in the Central Nile Delta is delineated [33], and the gas potential is evaluated at several fields, e.g. Abu Madi and El Qara Fields [34]. However, the detailed reservoir characterization and architecture of the producing zones are not well addressed that makes understanding the hydrocarbon flow across the reservoir significantly difficult. In the present study, a detailed methodology to characterize the pay zones of Abu Madi into HFUs and calculate their flow capacity is described using permeability-derived from multiple linear regression of available well log data. Such information is crucial for understanding the hydrocarbon flow across the reservoir and helps improving the efficiency of the static reservoir models.

2. Data Set and Methods

The key reservoir characteristics and dominant HFUs in Abu Madi pay zones

are investigated using 8 well logs (AMD1 to AMD6, AMD8 and AMD9) and SCAL data of two wells (AMD2 and AMD5). These wells are located in the Middle Delta area that extends up to Mansoura city (**Figure 1**). In all wells, the available logs involve Gamma ray, Neutron porosity, bulk density, shallow and deep resistivity, and caliper. Sonic log is only reported for AMD2 and AMD4 wells. To accomplish the objective of the present study, the integration between well logs and core data is properly manipulated. Among the various logging techniques currently in use, the reservoir petrophysical properties in Abu Madi pay zones are derived using the interpretation procedures illustrated in the flow chart of **Figure 2**.

2.1. Petrophysical Calculations

Lithological composition is formulated either as three mineral components (sandstone, siltstone, and clay) using density and neutron logs or four minerals components (sandstone, limestone, dolomite, and clay) where density, neutron, sonic, and photo electric effect (PEF) logs are available [35]. An accurate shale volume estimation is essential for porosity and fluid saturation corrections because its effect on the calculations of these parameters. In addition, shale volume is essential for the determination of the net pay thickness and N/G ratio, an essential parameter in volumetric calculation of hydrocarbon reserve. Shale volume is calculated using several methods including gamma ray [36], shale resistivity index (Z) (Schlumberger, 2007), and neutron-density method [35]. **Table 1** summarizes the mathematical relations applied for Vshale calculations and other petrophysical properties in the present analysis. To calculate a reliable porosity estimate, both density and neutron porosity corrected for shale content are calculated [37] and the resulting values are geometrically averaged to yield the density-Neutron porosity ($\Phi_{N\text{-}D}$) [7] [38]. Due to its flexibility to involve the effect of various parameters such as lithological composition and others, Indonesia equation is utilized to calculate water saturation. Typically, hydrocarbon saturation (Sh) is calculated as a function of Sw according to the simple relation "Sh = 1 − Sw".

2.2. Permeability Calculation

In the present study, both micro and macro scale categories are tested to determine the best model that fits optimum prediction of permeability in the study area. Timur and Schlumberger models [25] are respectively described mathematically in **Table 1**. MLR analysis is a model-based technique and has been suggested as a useful tool for correlating the permeability to rock properties if the number of variables is more than two [39]. In MLR, various log measurements (GR, TNPH, RT, and RHOB) are utilized to predict permeability using the corresponding core permeability as a constraint. MLR prediction model is first built and calibrated using core permeability and well logs data taken every 1 ft in reservoir interval of AMD2 well and subse-

quently validated using core permeability of AMD5 well. In addition the same core data is used to compare the MLR permeability predictions with those of Timur and Schlumberger models to determine the model with best performance.

Table 1. The mathematical relations applied to calculate the petrophysical parameters for Abu Madi reservoir, Nile Delta.

Parameter	Equation	Reference
Shale Volume (Vsh) Using Gamma Ray Log	$I_{GR} = \frac{GR_{\log} - GR_{\min}}{GR_{\max} - GR_{\min}}$ $V_{sh} = 0.083\left(2^{3.7*I_{GR}} - 1\right)$	Bassiouni, 1994
Shale Volume (Vsh) Using Resistivity Log	$Z = \frac{R_{clay}}{R_t} \times \frac{\left(R_{clean} - R_t\right)}{\left(R_{clean} - R_{clay}\right)}$ For R_t greater than 2*R_{clay} then $V_{shRes} = 0.5 \times \left(2 \times Z\right)^{0.67 \times (z+1)}$ Otherwise, $V_{shRes} = Z$	Schlumberger, 2007
Density Porosity (ϕ_{Dcorr})	$\phi_{Dcorr} = \left(\frac{\rho_{ma} - \rho_b}{\rho_{ma} - \rho_f}\right) - Vsh\left(\frac{\rho_{ma} - \rho_{sh}}{\rho_{ma} - \rho_f}\right)$	Dresser, 1975
Neutron Porosity (ϕ_{Ncorr})	$\phi_{Ncorr} = \phi_N - \left[\left(\frac{\phi_{Nsh}}{0.45}\right) \times 0.30 \times V_{sh}\right]$	Dresser, 1975
Average Porosity (ϕ_{N-D})	$\phi_{N-D} = \sqrt{\frac{\phi^2_{Ncorr} + \phi^2_{Dcorr}}{2.0}}$	Salley, 1998; Asqith & Krygowski, 2004
Water Saturation (Sw) (Poupon-Leveaux)	$\frac{1}{\sqrt{R_t}} = \left(\sqrt{\frac{\phi^m}{a \times R_w}} + \frac{V_{sh}^{\left(1 - \frac{V_{sh}}{2}\right)}}{\sqrt{R_{sh}}}\right) \times S_w^{\frac{n}{2}}$	Schlumberger, 2007
Hydrocarbon Saturation (S_h)	$S_h = 1 - S_W$	Bassiouni, 1994
Residual Hydrocarbon Saturation (S_{hr})	$S_{xo} = \sqrt{\frac{F * R_{mf}}{R_{XO}}}$ $S_{hr} = 1 - S_{xo}$	Bassiouni, 1994
Permeability (k) Timur Model	$K = 8581 * \frac{\phi^{4.4}}{Swirr^2}$	Brock, 1986
Permeability (k) Schlumberger Model	$K = 10000 * \frac{\phi^{4.5}}{Swirr^2}$	Brock, 1986
Flow Capacity (Fm)	$F_m = \frac{\sum_{i=1}^{m} k_i h_i}{\sum_{i=1}^{n} k_i h_i}; m = 1, \ldots, n$	Gunter, *et al.*, 1997
Storage Capacity (Φm)	$\Phi_m = \frac{\sum_{i=1}^{m} \Phi_i h_i}{\sum_{i=1}^{n} \Phi_i h_i}; m = 1, \ldots, n$	Gunter, *et al.*, 1997

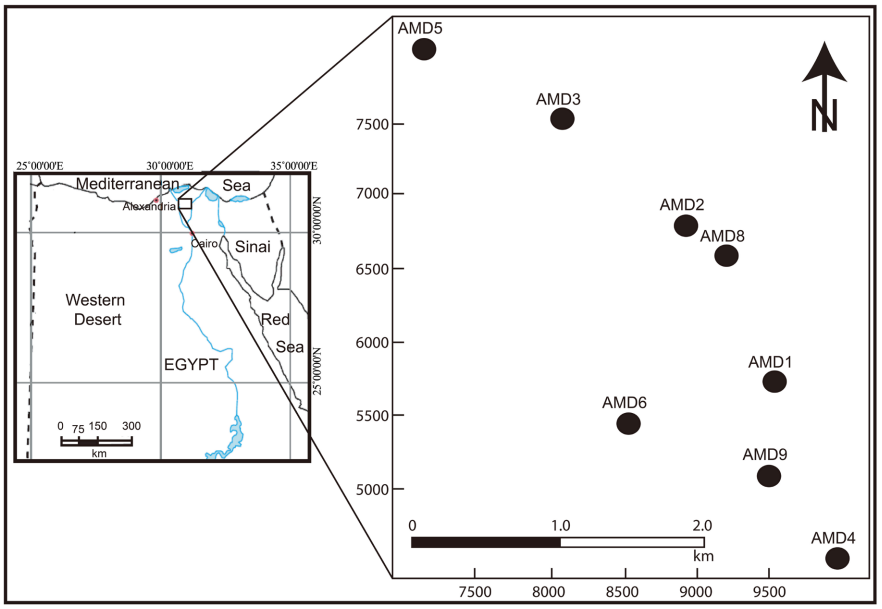

Figure 1. Location map to the study area showing well sites.

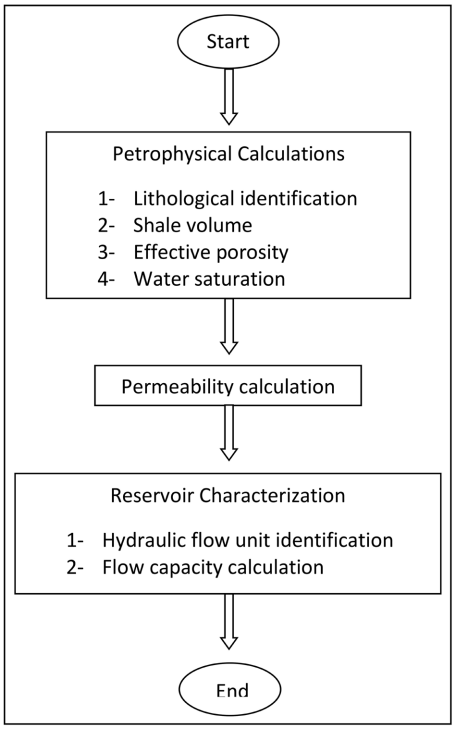

Figure 2. A flow chart of the applied methods.

2.3. Reservoir Characterization

This involves Hydraulic Flow Unit (HFU) identification and Reservoir Flow Capacity (RFC) calculation. Reservoir flow units can be identified using the modified Lorenz plot method described by Gunter *et al.* [40]. This method involves calculating the cumulative flow capacity (Fm) (Table 1), and then defining the cumulative storage capacity Φm (Table 1). Such calculations are applied for each depth

interval through the studied wells. The plot of Fm versus Φm identifies the hydraulic flow units through the change in slope. Such analysis enables tracking the identified hydraulic flow units developed throughout the reservoir, both vertically and spatially. RFC is characterized based on the statistics of calculated permeability in the different flow units and their corresponding thickness throughout the studied well. Mathematically, RFC for a specific flow unit is approximated by multiplying the average calculated permeability (D) by the measured thickness (ft). On local scale, RFC can be characterized into categories based on the calculated capacity that falls between very poor and excellent RFC. All calculations and data analysis have been accomplished using IP version 3.4 software [35].

3. Results and Discussion

The log data of eight wells penetrating the reservoir pay intervals are evaluated qualitatively for consistency. In addition, the reservoir zones are quantitatively evaluated for clay volume, porosity, and fluid content. A sample of log analysis and preliminary interpretation is presented in **Figure 3**. For each well, several statistical analyses are conducted to reveal the trends in each property distribution, vertically and spatially. Results of these statistical analyses on pay results for porosity, water saturation, volume of clay, residual hydrocarbon saturation, movable hydrocarbon saturation and net/gross ratio are presented in **Table 2**. In the present study, delineation of net pay zones is accomplished using reasonable cutoffs values (clay volume: 20%, porosity: 15%, and Sw: 40%), selected based on the conventions with guidance of the operating companies. The net pay thickness for all available wells (**Table 2**) shows that the gross thickness of the pay zones varies between 18.3 ft at AMD9 well and 168 ft at AMD2 well with an average thickness of 112 ft. Alternatively, the net pay thickness of these wells are respectively 11.3 and 156 ft with an average pay thickness of 98 ft. The Net-to-Gross ratio calculated for these zones showed the lowest values at AMD9 well (0.62) while the highest value is reported at AMD1 well (0.98). Generally, the thick intervals are encountered at the central parts of the mapped area and decrease gradually towards the Northwest and Southeast directions.

A simple statistical analysis for porosity measured at all wells (**Table 2**) indicates that porosity experienced insignificant changes as indicated by the low average standard deviation (1.1), with a substantial vertical variations within the reservoir interval as observed across AMD3 and AMD9 wells, where the standard deviation for these wells reports 5.5. Results in **Table 1** show a relatively good average reservoir porosity that varies between 26.5% (AMD9 well) and 20.9% (AMD3 well). The average calculated reservoir porosity of all wells reported 23.5%, and most of the reported porosity values are falling close to this value indicating lower standard deviation (1.1%). Such porosity pattern may indicate the presence of at least 2 channels system passing through the study area and are separated by numerous point bars or levees. In channel systems, the sand content associating higher porosity values normally increases relative to silt

and clay contents, while point bars and levees usually have higher silt and clay contents (Figure 3). Due to its physical behavior, shale content strongly affects the calculations of water saturation and porosity [41]. Therefore, accurate clay volume estimates are important for the compulsory Sw and porosity corrections. The average Vclay varies between 0.05% at AMD8 well and as much as 12% at AMD6 well with an average value of 5.9% throughout the tapped reservoir intervals. The Vclay shows moderate changes in most wells as the standard deviation usually falls between 0.06% to 1.3%, but such variations markedly increase in AMD3, AMD4, and AMD5 wells to report 1.6%, 1.65%, and 1.7% respectively.

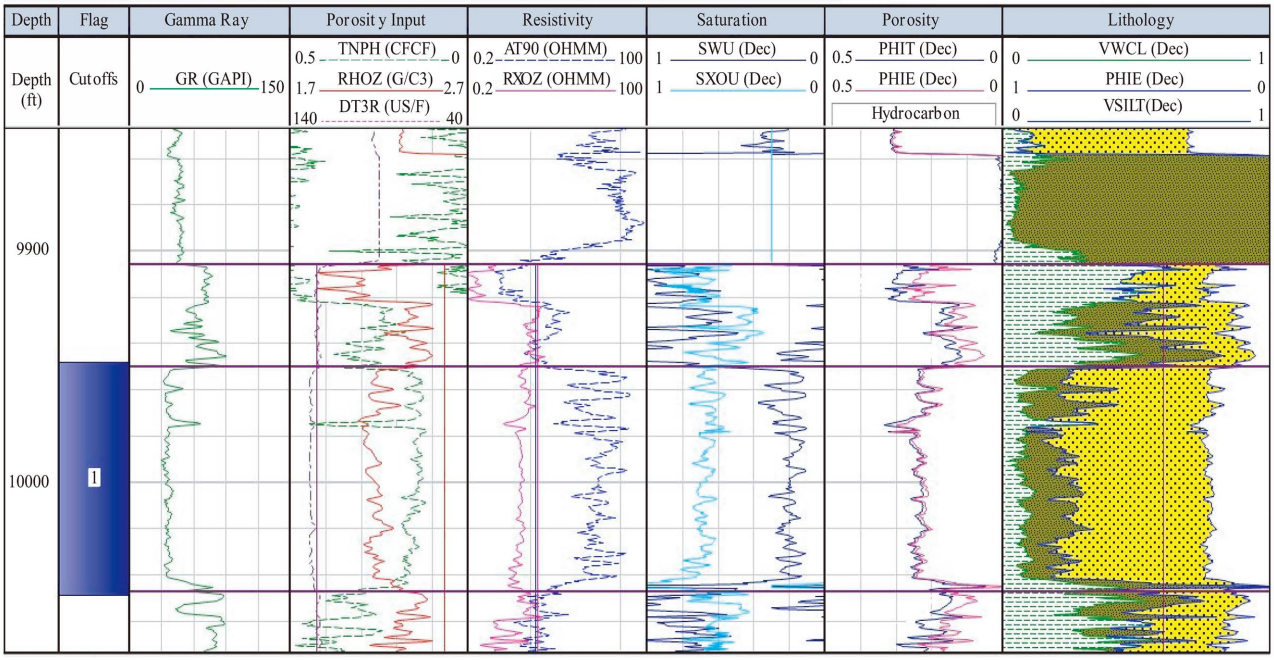

Figure 3. Log data and the interpretation of petrophysical parameters in AMD1 well.

Table 2. Results of the statistical analyses on the pay petrophysical parameters in Abu Madi reservoir, Nile Delta.

Petrophysical Parameters	Average Calculated Parameters at Wells								Net Pay Statistics			
	AMD1	AMD2	AMD3	AMD4	AMD5	AMD6	AMD8	AMD9	Min.	Max.	Avg.	StDev.
Porosity (%)	22.8	23.6	20.9	23.5	24.5	23.5	23	26.5	20.9	26.5	23.5	1.6
Clay Volume (%)	7.1	4	10.1	4.5	7	12	0.5	1.6	0.5	12.0	5.9	4.0
Water Saturation (SW, %)	20	22.6	21	23.2	20	24.2	36	26.4	20.0	36.0	24.2	5.2
Resid. HCSat (S_{HCr}, %)	32.4	36.7	51.7	21.7	47	33.4	31.9	35.7	21.7	51.7	36.3	9.3
Mov. HC (per Volume)	0.11	0.10	0.06	0.13	0.12	0.10	0.07	0.10	0.06	0.13	0.1	0.023
Net/Gross (%)	98.0	93.3	97.8	84.5	84.8	81.6	74.8	61.6	61.7	93.3	87.1	12.3

Water saturation and hydrocarbon mobility is typically determined to delineate potential permeable zones with movable hydrocarbon as a prerequisite for well development and production strategy. The reported average Sw of pay results is 24.2% with 5% standard deviation while the maximum Sw (36%) is reported in AMD8 well indicating spurious effects induced by such increase. The highest average water saturation could be attributed to the higher clay content dispersed within the reservoir sand. Generally, marked higher Sw values are reported in wells located in the Eastern part particularly near the NE and SE segments of the reservoir. The average movable hydrocarbon varies between 27.3% at AMD3 well and 55.1% at AMD4 well with average value 39.5% and standard deviation 9.7%. Such statistics indicate moderate changes in the average movable hydrocarbon calculated at different wells. Alternatively, the residual hydrocarbon calculated showed approximately inversed relationship to the average movable hydrocarbon at different wells (**Table 2**). The statistics of the net pay showed that the highest bulk volume (0.08) of water (BVW) is reported at AMD8 well while the lowest BVW (4%) was in AMD3 well.

3.1. Permeability Calculations

Permeability prediction is a key parameter for successful reservoir characterizations but unfortunately, its measurement is always a challenging task both technically and economically. In the present study, Timur and Schlumberger models are applied to calculate permeability in Abu Madi pay zones. Timur permeability correlates very well with Schlumberger permeability for AMD2 and AMD5 well (**Figure 4** Left). However, when compared to the core permeability at these wells low to moderate agreement is observed between the measured and calculated values (**Figure 4** Right). In both wells the calculated porosity showed a good agreement to the measured porosity in core samples (**Table 2**). Generally, in AMD2 well two trends are observed as the calculated permeability is overestimated where the core permeability fall below 1000 mD but is underestimated where the core permeability records over 1000 mD. Alternatively, in AMD5 well where permeability does not exceed a 1000 mD, the calculated permeability showed erratic responses to the measured permeability with notable large variations (more than double the values) between the measured and calculated values. Thus, reliable estimation of permeability cannot be pursued with these methods, and therefore MLR approach, as field scale data, is applied to predict permeability taking core permeability values as a reference for comparison.

Using core permeability and well log data recorded every 1 ft at the reservoir interval of AMD2 well, MLR model is developed to predict permeability using well log measurements, and subsequently the predicted values are validated using core permeability data of AMD5 well. As a function of GR, TNPH, RT, and RHOB readings, the permeability (K-value) can be calculated using MLR model as;

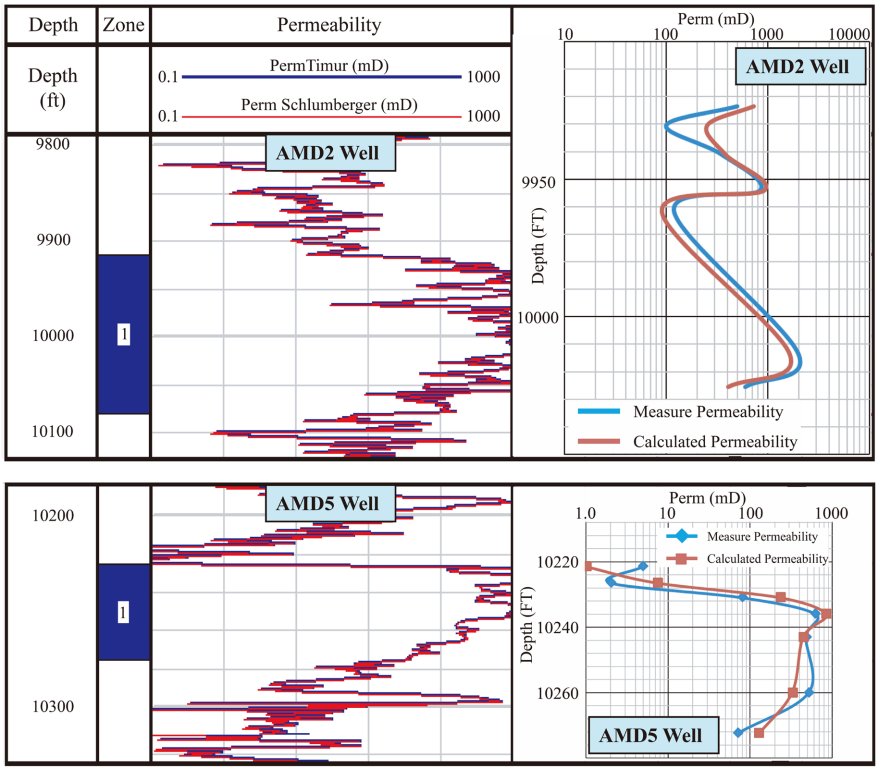

Figure 4. The permeability calculated by Timur and Schlumberger models (left) and a comparison between measured and calculated permeability (right) in AMD2 and AMD5 wells.

$$K = 10 \wedge \begin{pmatrix} 15.673177 - 1.2518737 * Log(GR) + 2.0795269 * Log(TNBH) \\ +1.1522252 * Log(RT) - 30.74073 * Log(RHOB) \end{pmatrix}$$

Accepting the match between calculated and measured permeability in AMD5 well shown in **Figure 5**, the MLR model is considered calibrated and capable to predict K-values in the other wells using log data records. **Table 3** presents the results of the average calculated permeability in the reservoir interval of all wells penetrating Abu Madi Formation in the Nile Delta and the spatial distribution of the permeability is presented in **Figure 6**. The results of calculated permeability show that Abu Madi Formation has a relatively good permeability (hundreds of mD) in all wells except AMD8 well where it reports 89 mD. The permeability distribution map (**Figure 6**) shows marked decrease in the Mideast region near AMD1 and AMD8 wells. Such observation supports the assumption of the development of a point bar at this region of the study area adjacent to the course of a paleo-channel where the other wells are located.

3.2. Hydraulic Flow Units (HFU) Characterization

For each well, the Modified Lorenz plot (Fm versus Φm,) is constructed and the change in slope delineates the HFUs in this well [40]. These plots enable characterizing the developed HFU vertically while the lateral extension of each HFU is pursued through well-to-well correlation, as presented in **Figure 7**. Such analysis

Table 3. The average calculated permeability for the available wells in Abu Madi reservoir, Nile Delta.

Well	AMD1	AMD2	AMD3	AMD4	AMD5	AMD6	AMD8	AMD9
Avg. K (mD)	234.7	767.8	569.0	1399.3	609.4	594.8	89	478.5

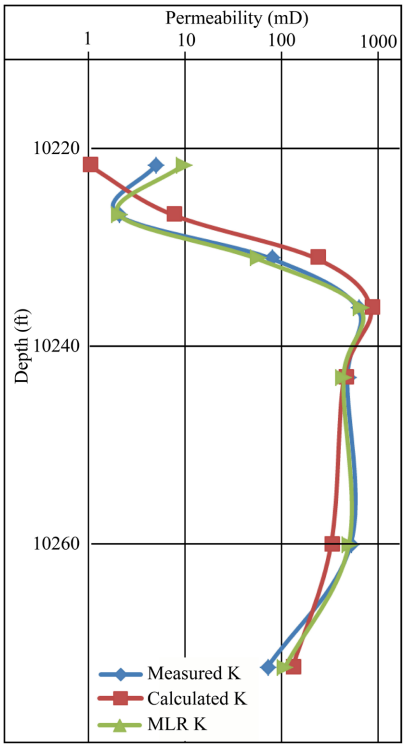

Figure 5. The measured core permeability compare to both calculated Timur permeability and MLR permeability at various depth in pay zone of AMD5 well.

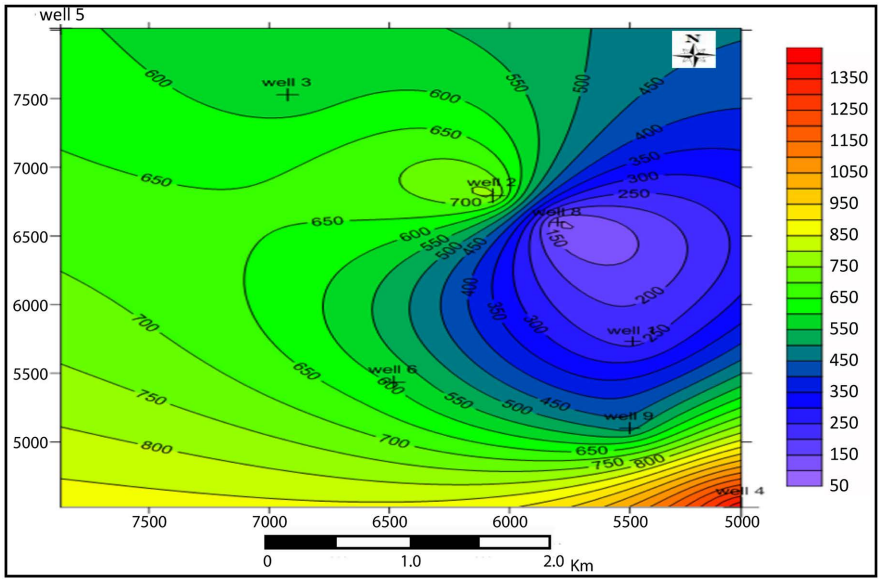

Figure 6. The spatial distribution of average calculated permeability in Abu Madi reservoir, Nile Delta.

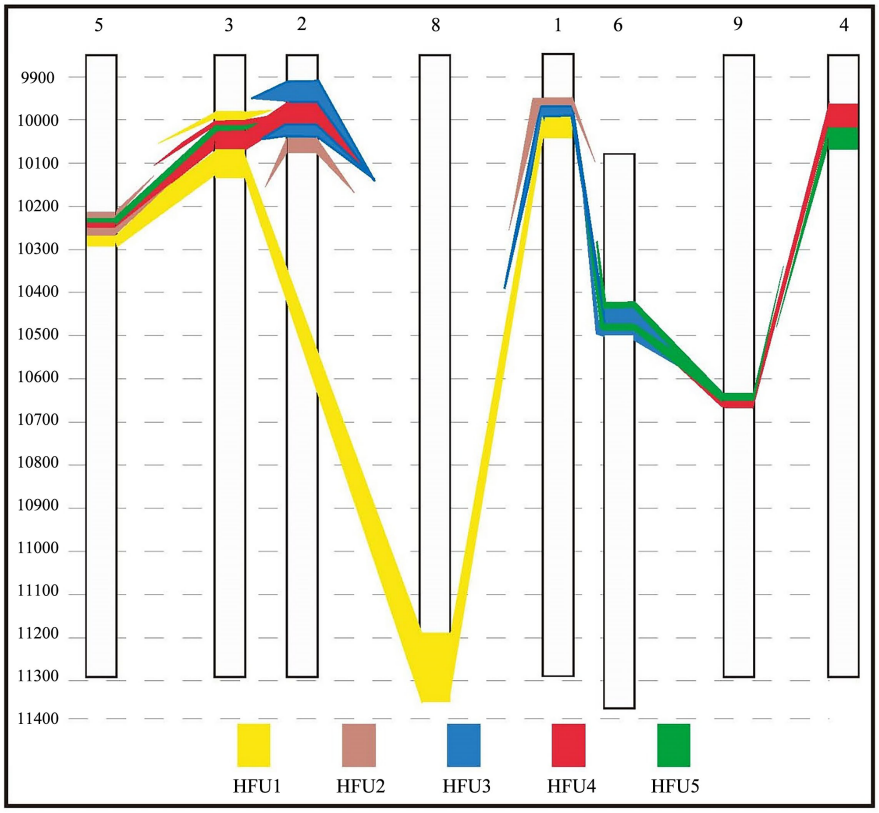

Figure 7. Well-to-well correlation showing the lateral extension of the developed HFUs across Abu Madi reservoir, Nile Delta.

provides indirect tool to check the accuracy of the Modified Lorenz plot in identifying the flow units in each well. Abu Madi Formation showed various HFUs distributed throughout the reservoir. Each HFU is statistically analyzed and the results are tabulated in **Table 4**. The statistical parameters indicate reservoir heterogeneity through the studied sedimentary section. Data clustering of **Table 4** indicated the development of at least 5 HFUs with various hydraulic capacities. These hydraulic capacities of the HFUs can be characterized in terms of the prevailed average permeability (**Table 4**). Accordingly, the developed HFUs is categorized into five orders according to its hydraulic capacity that extend between 1 for units with poor capacity (K < 220 mD) and 5 for units with excellent capacity (K > 1270 mD). Based on these criteria the developed HFUs are correlated among wells and the results are presented in **Figure 7**.

HFU1 is encountered at 4 wells (AMD1, AMD3, AMD5, AMD8) distributed along the reservoir with a thickness ranges between 19 ft at AMD5 well and 180 ft at AMD8 well. **Figure 8** (upper) shows the thickness distribution map of the HFU1 in study area, where the thick zone occurs at the Northeastern part and decrease gradually to disappear near the middle parts. The average permeability in the studied wells varies between 77 mD in AMD8 well and 220 mD in AMD1 well, with corresponding standard deviation of 30 and 215 mD respectively (**Table 4**). In addition, the hydraulic flow capacity (HFC = [Thickness (ft)*Hydraulic con-

ductivity (mD)]/1000) of HFU1 indicates that AMD3 well has the highest flow capacity among the studied wells, but the associating high standard deviation indicates reservoir heterogeneity that results in tortuous flow regimes at this location. Thus, it is expected that the flow regime in AMD8 well, with lower permeability, lower standard deviation, and a relatively higher flow capacity, is probably encountering lower tortuosity. HFU2 occurs in three wells (AMD1, AMD2, and AMD5) with thickness between 16 ft. in AMD5 well and 33 ft in AMD2 well. The thickness distribution map (**Figure 8**, lower) shows that HFU2 predominates the middle part of the reservoir and decreases gradually towards the Northeast and disappears near the Southern parts. The average permeability calculated in this unit falls around 300 mD with a standard deviation as low as 134 mD in AMD5 well to 819 mD in AMD2 well (**Table 4**). Despite the high standard deviation of permeability in AMD2 wells, there is a marked increase in its hydraulic flow capacity (13.2 D.ft) compared to the HFC in AMD-1 well (5.3 D.ft) and AMD5 well (4.6 D.ft).

HFU3 is also encountered at 3 wells (AMD1, AMD2, AMD6) with a thickness varies between 26 ft at AMD1 well and 81 ft at AMD2 well. The thickness distribution map (**Figure 9**, upper) reveals a gradual decrease in the HFU3 thickness towards the Northwest and Southeast, but the notable increase in thickness towards the Northeast and Southwest is not real and presents contouring artifacts as it is not supported by real field measurements. The average hydraulic conductivity reported in this unit falls around 500 - 600 mD with a standard deviation as small as 365 mD in AMD1 well to 600 mD at AMD2 well (**Table 4**). HFU 3 reported calculated flow capacity between 12.5 D.ft in AMD1 well and 50 D.ft in AMD2 well, representing a transition stage between the low flow capacity in HFU1 and HFU 2 and the high flow capacity in HFU4 and HFU5 (**Table 4**). HFU4 occurs in 5 wells (AMD2, AMD3, AMD4, AMD5, and AMD9) with a thickness between 13 ft. in AMD9 well and 59 ft. in AMD4 well. The thickness distribution map of HFU4 (**Figure 9**, lower) shows a relatively full coverage through the study area with thick zones (~60 ft. thick) encountered at the Northwest and Southeast separated by HFU3-zone of less than 20 ft thick. HFU4 presents a high flow capacity unit with calculated permeability between 820 mD at AMD5 well and 1270 mD at AMD2 well (**Table 4**). The permeability variations in individual wells showed a marked change as indicated by the calculated standard deviation that varies between 370 mD in AMD5 well and 1470 mD in AMD4 well. The calculated flow capacity reported values as low as 14 D.ft in AMD5 and AMD9 wells but increase to report 70 D.ft in AMD2 and AMD4 wells (**Table 4**). HFU5 is encountered at 5 wells (AMD3, AMD4, AMD5, AMD6, and AMD9) with the majority of these wells having thickness of approximately 5 ft (AMD3, AMD5, and AMD9 wells) but a relatively thick zone (53 ft.) is also found at AMD4 well. This is clearly depicted in the thickness distribution map (**Figure 10**) where these thick zones are found at the South-Southwestern part of the reservoir. The hydraulic conductivity of this unit shows absolutely higher

values and typically varies between 2250 mD (AMD6 well) and 4100 mD (AMD3 well). Despite this high calculated permeability, it is expected that the flow regime suffers a considerable tortuosity as indicated by the high standard deviation of permeability that falls between 2200 mD to 3000 mD (**Table 4**). Due to the small thickness, the HFC calculated in most wells fall between 15 and 20 D.ft, while considerably large values (138 D.ft) are calculated at AMD4 well.

Figure 8. The thickness distribution map for both HFU1 (upper) and HFU2 through Abu Madi reservoir, Nile Delta.

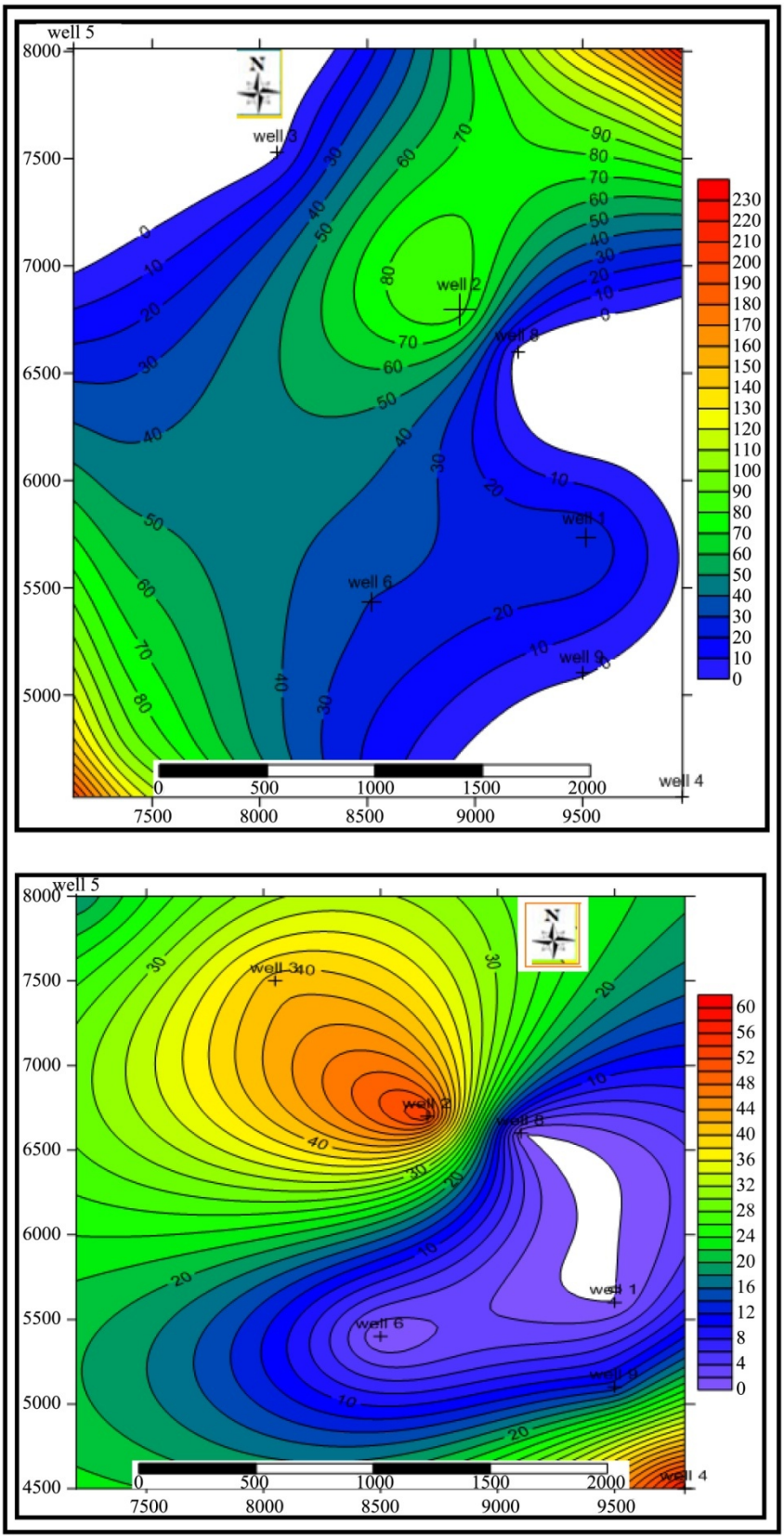

Figure 9. The thickness distribution map of HFU3 (upper) and HFU4 (lower) through Abu Madi reservoir, Nile Delta.

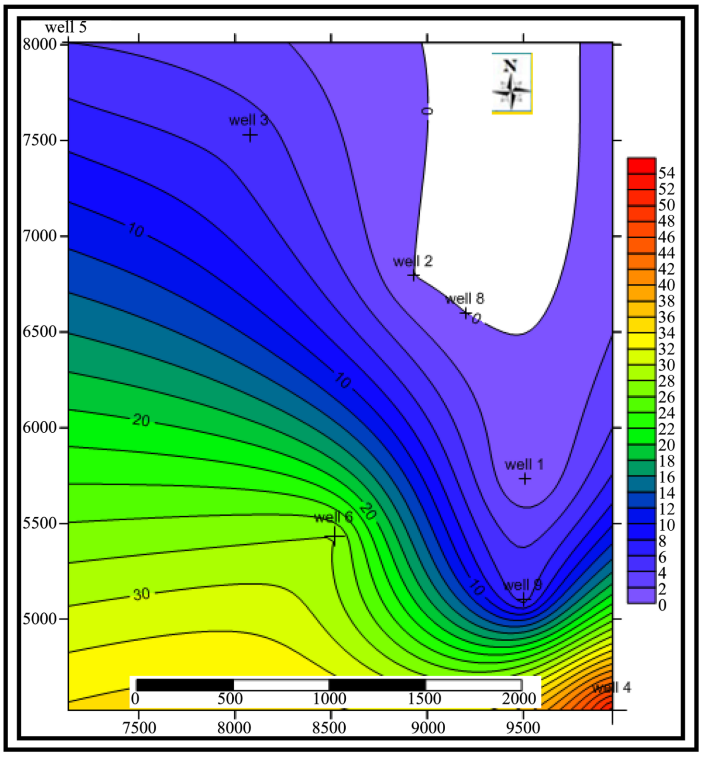

Figure 10. The thickness distribution map of HFU5 through Abu Madi reservoir, Nile Delta.

Table 4. The HFUs statistics and the calculated reservoir flow capacity for Abu Madi reservoir, Nile Delta.

Wells	HF1				HFU2				HFU3			
	Thick (ft.)	K avg (mD)	Std Dev	HFC	Thick (ft.)	K avg (mD)	Std Dev	HFC	Thick (ft.)	K avg (mD)	Std Dev	HFC
WKh-1	55.0	220.0	215.0	12.1	20.0	266.0	310.0	5.3	26.0	482.0	365.0	12.5
WKh-2	-	-	-	-	33.0	399.0	819.0	13.2	81.0	623.0	601.0	50.5
WKh-3	90.0	178.0	252.0	16.0	-	-	-	-	-	-	-	-
WKh-4	-	-	-	-	-	-	-	-	-	-	-	-
WKh-5	19.0	126.0	100.0	2.4	16.0	285.0	134.0	4.6	-	-	-	-
WKh-6	-	-	-	-	-	-	-	-	30.0	490.0	410.0	14.7
WKh-8	150.0	77.0	30.0	11.6	-	-	-	-	-	-	-	-
WKh-9	-	-	-	-	-	-	-	-	-	-	-	-

Wells	HFU4				HFU5				Sum HFC
	Thick (ft.)	K avg (mD)	Std Dev	HFC	Thick (ft.)	K avg (mD)	Std Dev	HFC	
WKh-1	-	-	-	-	-	-	-	-	30.0
WKh-2	54.0	1268.0	883.0	68.5	-	-	-	-	132.1
WKh-3	41.0	1059.0	1309.0	43.4	5.0	4120	2238	20.6	80.0
WKh-4	59.0	1133.0	1469.0	66.8	53.0	2611	2488	138.4	205.2
WKh-5	18.0	820.0	373.0	14.8	4.0	3953	2757	15.8	37.5
WKh-6	-	-	-	-	28.0	2270	2975	63.6	78.3
WKh-8	-	-	-	-	-	-	-	-	11.6
WKh-9	8.5	998.0	882.0	8.5	5.0	3673	1358	18.4	26.8

The total flow capacity at each well reflects the reservoir flow capacity at the location of this well. The calculated reservoir flow capacity within Abu Madi reservoir (Table 4) might be classified into 4 categories. The first category includes the lowest flow capacity (~11 D.ft) and is well-presented in AMD8 well, while the second category involves wells with capacity around 30 D.ft (AMD1, AMD5, and AMD9 wells). The third category involves wells with high calculated capacity that falls close to 80 D.ft as reported in AMD3 and AMD6 wells. The fourth category represents the highest reported flow capacity with values typically greater than 130 D.ft that was calculated in AMD2 and AMD4 wells (Table 4). Generally, HFU 4 and HFU5 is responsible for the high total reservoir flow capacity in categories 3 and 4, while HFU5 is particularly responsible for the high flow capacity encountered at AMD4 well (205 D.ft) and AMD6 well (78 D.ft). Generally, wells located in the Northwestern part of the reservoir (AMD5, AMD3, AMD2, and AMD1 wells) develop 3 HFUs that relatively vary from the two HFUs (Figure 7) developed in wells of the Southeast (AMD6, AMD9, and AMD4 wells). Only one well (AMD8 well) develops a single HFU that occupies the central part of the reservoir and separates the two sets of HFUs. Generally, the Southeastern part of the reservoir is characterized by good flow capacity as indicated by the development of higher HFUs (3, 4, and 5) compared to the Northeastern part with lower HFUs (1, 2, 3, and 4).

4. Conclusion

The petrophysical analysis and reservoir characterization of Abu Madi Formation indicated the presence of at least 2 paleo-channel systems, separated by numerous point bars or levees that constitute the important pay zones of Abu Madi Formation. In addition, the high hydrocarbon reserve wells are aligned at shallow depth pay zone while the low reserve wells are encountered in the deeper parts of the reservoir indicating upward migration towards the shallow parts and hydraulic continuity across the reservoir. The higher shale content sometimes hinders the hydraulic continuity through the pay zone and, therefore, some shallow pay zones may show low reserve. After testing the performance of Timur and Schlumberger models to predict permeability using core data, multi linear regression approach using GR, TNPH, Rt, and RHOB records is applied and the predicted permeability values showed a good match to core measurements. Using the predicted permeability, hydraulic flow units are characterized through the reservoir. The developed HFUs are categorized according to its hydraulic capacity from 1 for units with poor capacity ($K < 220$ mD) to 5 for units with excellent capacity ($K > 1270$ mD). The wells in the Northwestern part of the reservoir develop 3 HFUs but the Southeastern wells develop 2 HFUs characterized by good flow capacity. The central part of the reservoir reported only one HFU. Such characterization data are crucial for reservoir development and forecasting reservoir performance using modeling techniques.

Conflicts of Interest

The authors declare no conflicts of interest regarding the publication of this paper.

References

[1] Harris, D.G. and Hewitt, C.H. (1977) Synergism in Reservoir Management—The Geologic Perspective. *Journal of Petroleum Technology*, **29**, 761-770. https://doi.org/10.2118/6109-PA

[2] Amaefule, J.O., Altunbay, M.H., Tiab, D., Kersey, D.G. and Keelan, D.K. (1993) Enhanced Reservoir Description Using Core and Log Data to Identify Hydraulic (Flow) Units and Predict Permeability in Uncored Intervals/Wells. *SPE Annual Technical Conference and Exhibition*, Houston, 3-6 October, Paper No: 26436. https://doi.org/10.2118/26436-MS

[3] Keelan, D.K. (1982) Core Analysis for Aid in Reservoir Description. *Journal of Petroleum Technology*, **34**, 2483-2490. https://doi.org/10.2118/10011-PA

[4] Sneider, R.M., King, H.R., Hawkes, H.E. and Davis, T.B. (1983) Methods for Detection and Characterization of Reservoir Rock, Deep Basin Gas Area, Western Canada. *Journal of Petroleum Technology*, **35**, 1725-1734. https://doi.org/10.2118/10072-PA

[5] Worthington, P.F. and Cosentino, L. (2003) The Role of Cut-Offs in Integrated Reservoir Studies. *SPE Annual Technical Conference and Exhibition*, Denver, 5-8 October, Paper No: 84387. https://doi.org/10.2118/84387-MS

[6] Teh, W., Willhite, G.P. and Doveton, J.H. (2012) Improved Reservoir Characterization in the Ogallah Field Using Petrophysical Classifiers within Electrofacies. *SPE Improved Oil Recovery Symposium*, Tulsa, 14-18 April, Paper No: 154341. https://doi.org/10.2118/154341-MS

[7] Selley, R.C. (1998) Elements of Petroleum Geology. Academic Press, London, United Kingdom, 470 p.

[8] Taghavi, A.A. (2005) Improved Permeability Estimation through Use of Fuzzy Logic in a Carbonate Reservoir from Southwest, Iran. *SPE Middle East Oil and Gas Show and Conference*, Kingdom of Bahrain, 12-15 March, Paper No: 93269. https://doi.org/10.2118/93269-MS

[9] Svirsky, D., Ryazanov, A. and Pankov, M. (2004) Hydraulic Flow Units Resolve Reservoir Description Challenges in a Siberian Oil Field. *SPE Asia Pacific Conference on Integrated Modelling for Asset Management*, Kuala Lumpur, 29-30 March 2004, Paper No: 87056. https://doi.org/10.2118/87056-MS

[10] Ebanks Jr., W.J. (1987) Flow Unit Concept-Integrated Approach to Reservoir Description for Engineering Projects, abst. *AAPG Bulletin*, **71**, 551-552.

[11] Ebanks, W., Scheihing, M. and Atkinson, C. (1992) Flow Units for Reservoir Characterization. In: Morton-Thompson, D. and Woods, A.M., Eds., *Development Geology Reference Manual*, American Association of Petroleum Geologists Methods in Exploration Series 10, 282-284.

[12] Abbaszadeh, M., Fujii, H. and Fujimoto, F. (1996) Permeability Prediction by Hydraulic Flow Units—Theory and Applications. Society of Petroleum Engineers.

[13] Guo, G., Diaz, M.A., Paz, F.J., Smalley, J. and Waninger, E.A. (2007) Rock Typing as an Effective Tool for Permeability and Water-Saturation Modeling: A Case Study in a Clastic Reservoir in the Oriente Basin. *SPE Reservoir Evaluation and Engineering*, **10**, 730-739. https://doi.org/10.2118/97033-PA

[14] Carman, P.C. (1956) Flow of Gases through Porous Media. Academic Press Inc., New York.

[15] Amyx, J.W., Bass, D.M. and Whiting, R.L. (1960) Petroleum Reservoir Engineering. McGraw-Hill Book Co., New York.

[16] Hearst, J.R., Nelson, P.H. and Paillet, F.L. (2000) Well Logging for Physical Properties. John Wiley and Sons, New York.

[17] Timur, A. (1968) An Investigation of Permeability, Porosity and Residual Water Saturation Relationships for Sandstone Reservoirs. *The Log Analyst*, **9**, 10.

[18] Kolodzie Jr., S. (1980) Analysis of Pore Throat Size and Use of the Waxman-Smits Equation to Determine OOIP in Spindle Field, Colorado. *SPE Annual Technical Conference and Exhibition*, Dallas, 21-24 September 1980, SPE 9382. https://doi.org/10.2118/9382-MS

[19] Pittman, E.D. (1992) Relationship of Porosity and Permeability to Various Parameters Derived From Mercury Injection-Capillary Pressure Curves for Sandstone. *American Association of Petroleum Geologists Bull*, **76**, 191-198.

[20] Lee, S.H., Kharghoria, A. and Datta-Gupta, A. (2002) Electrofacies Characterization and Permeability Predictions in Complex Reservoirs. *SPE Reservoir Evaluation and Engineering*, **5**, 237-248. https://doi.org/10.2118/78662-PA

[21] Taware, S.V., Taware, A.G., Sinha, A.K., Jamkhindikar, A., Talukdar, R. and Datta-Gupta, A. (2008) Integrated Permeability Modeling Using Wireline Logs, Core and DST Data in a Deepwater Reservoir. Society of Petroleum Engineers, Dallas. https://doi.org/10.2118/113599-MS

[22] Mohaghegh, S., Balan, B. and Ameri, S. (1997) Permeability Determination from Well Log Data. *SPE Formation Evaluation*, **12**, 170-174. https://doi.org/10.2118/30978-PA

[23] Al-anazi, A.F. and Gates, I.D. (2010) Support-Vector Regression for Permeability Prediction in a Heterogeneous Reservoir: A Comparative Study. *SPE Reservoir Evaluation and Engineering*, **13**, 485-495.

[24] Perez, H.H., Datta-Gupta, A. and Mishra, S. (2003) The Role of Electrofacies, Lithofacies, and Hydraulic Flow Units in Permeability Predictions from Well Logs: A Comparative Analysis Using Classification Trees. Society of Petroleum Engineers. https://doi.org/10.2118/84301-MS

[25] Brock, J. (1986) Applied Open-Hole Log Analysis. Volume 2, Gulf Publishing Company, Houston.

[26] Mohammadmoradi, P. and Kantzas, A. (2016) Pore-Scale Permeability Calculation Using CFD and DSMC Techniques. Society of Petroleum Engineers, Dallas. https://doi.org/10.1016/j.petrol.2016.07.010

[27] Xue, G., *et al.* (1997) Optimal Transformations for Multiple Regression: Application to Permeability Estimation to Permeability Estimation from Well Logs. https://doi.org/10.2118/35412-PA

[28] Iturrarán-Viveros, U. and Parra, J.O. (2013) Permeability and Porosity from Integrated Multiattributes and Well Log Data Using Smooth Regression: Application to a South Florida Aquifer. Society of Exploration Geophysicists, Doc. ID: SEG-2013-0376.

[29] Al-Mudhafer, W.J. (2014) Using Generalized Linear Regression of Multiple Attributes for Modeling and Prediction the Formation Permeability in Sandstone Reservoir. https://doi.org/10.4043/25158-MS

[30] Saner, S., Kissami, M. and Al-Nufaili, S. (1997) Estimation of Permeability from

Well Logs Using Resistivity and Saturation Data. https://doi.org/10.2118/26277-PA

[31] Rios, E.H., de Vasconcellos Azeredo, R.B., Moss, A.K., Pritchard, T.N. and Domingues, A.B.G. (2015) Estimating the Permeability of Carbonate Rocks by Principal Component Regressions of NMR and MICP Data. Society of Petrophysicists and Well-Log Analysts, Doc. ID: SPWLA-2015-KKK.

[32] Rizzini, A., Vezzani, F., Goceccetta, V. and Milad, G. (1976) Stratigraphy and Sedimentation of Neogene-Quaternary Section in the Nile Delta Area. *Marine Geology*, **27**, 327-348. https://doi.org/10.1016/0025-3227(78)90038-5

[33] El Khadrawy, A. and Elewa, A. (2017) Sequence Stratigraphic Framework of Late Miocene Abu Madi and Qawasim Formations, Central Nile Delta, Egypt. Offshore Mediterranean Conference, Doc. ID: OMC-2017-583.

[34] Nassar, M., Matresu, J., Talat, A. and Hasan, M. (2015) Abu Madi Reservoirs-Evaluation of Level-III Remaining Gas Potential, Abu Madi and El Qara Fields. Society of Petroleum Engineers, Dallas. https://doi.org/10.2118/175768-MS

[35] Schlumberger (2007) Schlumberger IP User Manual. PGL-Senergy, Ternan House, V. 3.4.

[36] Bassiouni, Z. (1994) Theory, Measurement and Interpretation of Well Logs. Textbook Series, Society of Petroleum Engineers (SPE), Vol. 4.

[37] Atlas, D. (1975) Log Interpretation Fundamentals. Dresser Atlas Division, Dresser Industries, Inc.

[38] Asquith, G. and Krygowski, D. (2004) Basic Well Log Analysis. 2nd Edition, The American Association of Petroleum Geologist, Tulsa, AAPG. Methods in Exploration Series No. 16, 244 p.

[39] Wendt, W.A., Sakurai, S. and Nelson, P.H. (1986) Permeability Prediction from Well Logs Using Multiple Regression. In: Lake, L.W. and Carroll, H.B., Eds., *Reservoir Characterization* I, Academic Press, Cambridge, 181.

[40] Gunter, G.W., Finneran, J.M., Hartmann, D.J. and Miller, J.D. (1997) Early Determination of Reservoir Flow Units Using an Integrated Petrophysical Method. Society of Petroleum Engineers. https://doi.org/10.2118/38679-MS

[41] Schlumberger (1972) Log Interpretation/Charts. Schlumberger Well Services Inc., Huston, Vol. 1, 113 p.